

Combining many-body methods and density-functional theory

Julien Toulouse

Université Pierre & Marie Curie and CNRS, Paris, France

Hybrids combining many-body methods and DFT

Goal: improve the accuracy of present-day DFT

① **Multiconfigurational hybrids** (MCSCF+DFT)

and **double hybrids** (MP2+DFT)

with B. Civalleri, H. J. Jensen, L. Maschio, A. Savin, K. Sharkas

→ static (or strong) correlation or self-interaction error

② **Range-separated hybrids** (lrRPA+srDFT)

with J. Ángyán, O. Franck, G. Jansen, E. Luppi, B. Mussard, P. Reinhardt, A. Savin, W. Zhu

→ van der Waals dispersion interactions

③ **Time-dependent range-separated hybrids** (lrBSE+srTDDFT)

with T. Helgaker, E. Rebolini, A. Savin, A. Teale

→ Rydberg, charge-transfer, double excitations

Multiconfigurational hybrids (MCSCF+DFT)

Multideterminant DFT based on a **linear** decomposition of e-e interaction

$$E_{\text{exact}} = \min_{\Psi} \left\{ \langle \Psi | \hat{T} + \hat{V}_{ne} + \lambda \hat{W}_{ee} | \Psi \rangle + \bar{E}_{\text{Hxc}}^{\lambda}[n_{\Psi}] \right\}$$

with the λ -complement density functional $\bar{E}_{\text{Hxc}}^{\lambda}[n]$

- Hartree and exchange contributions:

$$\bar{E}_{\text{Hx}}^{\lambda}[n] = (1 - \lambda)E_{\text{Hx}}[n]$$

- Correlation contribution:

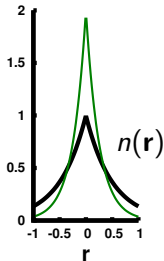
$$\bar{E}_c^{\lambda}[n] = E_c[n] - \lambda^2 E_c[n_{1/\lambda}] \approx (1 - \lambda^2)E_c[n]$$

- Approximations for Ψ and $E_{\text{xc}}[n]$

MCSCF: $\Psi = \sum_n c_n \Phi_n$

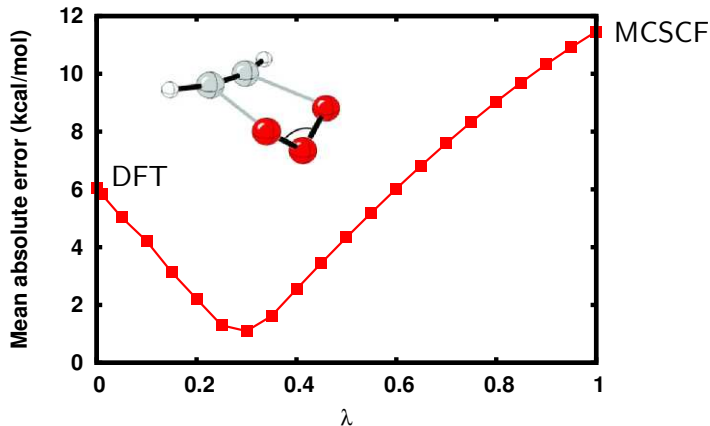
BLYP, PBE, etc...

$$n_{1/\lambda}(\mathbf{r}) = (1/\lambda)^3 n(\mathbf{r}/\lambda)$$



What value for the empirical parameter λ ?

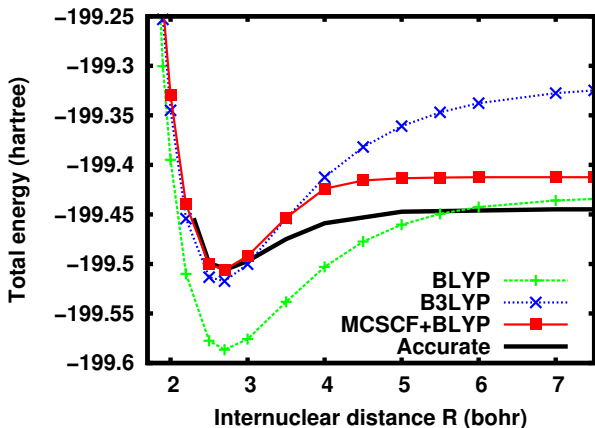
O3ADD6 set: 6 energy differences for cycloaddition reactions of ozone with ethylene or acetylene (aug-cc-pVTZ basis, BLYP functional):



⇒ We take $\lambda = 0.25$ as for usual hybrid functionals

Test of MCSCF+DFT on F_2 molecule

$\lambda = 0.25$, BLYP functional, cc-pVTZ basis:



⇒ **MCSCF+BLYP is as good as B3LYP at equilibrium and improves on it at dissociation**

Double hybrids (MP2+DFT)

- Start with linear decomposition of e-e interaction with single-determinant approximation

$$E_0 = \min_{\Phi} \left\{ \langle \Phi | \hat{T} + \hat{V}_{ne} + \lambda \hat{W}_{ee} | \Phi \rangle + \bar{E}_{\text{Hxc}}^{\lambda}[n_{\Phi}] \right\}$$

- Then, define the following perturbation theory:

$$E^{\alpha} = \min_{\Psi} \left\{ \langle \Psi | \hat{T} + \hat{V}_{ne} + \lambda \hat{V}_{\text{Hx}}^{\text{HF}} + \alpha \lambda \hat{W} | \Psi \rangle + \bar{E}_{\text{Hxc}}^{\lambda}[n_{\Psi}] \right\}$$

where $\lambda \hat{W} = \lambda \left(\hat{W}_{ee} - \hat{V}_{\text{Hx}}^{\text{HF}} \right)$ is a Møller-Plesset-type perturbation.

- At second order, we get a **double-hybrid approximation**:

$$E_{\text{xc}}^{\text{MP2+DFT}} = \lambda E_{\text{x}}^{\text{HF}} + (1 - \lambda) E_{\text{x}}[n] + (1 - \lambda^2) E_{\text{c}}[n] + \lambda^2 E_{\text{c}}^{\text{MP2}}$$

\Rightarrow **This provides a theoretical derivation of Grimme's double hybrids with only one parameter λ**

Performance of one-parameter double hybrids

$$E_{xc}^{\text{MP2+DFT}} = \lambda E_x^{\text{HF}} + (1 - \lambda) E_x[n] + (1 - \lambda^2) E_c[n] + \lambda^2 E_c^{\text{MP2}}$$

- For MP2+BLYP, optimization of λ on sets of molecular atomization energies and reaction barrier heights leads to $\lambda \approx \mathbf{0.65}$, corresponding to a fraction $\lambda^2 \approx 0.42$ of MP2 correlation.
- Inclusion of MP2 correlation allows one to use a **larger fraction of HF exchange**, which reduces the self-interaction error.
- Like the two-parameter double hybrids, the one-parameter double hybrids **reach near chemical accuracy (1-2 kcal/mol)** on thermochemistry properties for **systems without important static correlation effects**.
- For molecular crystals, double hybrids do not improve over MP2.

Sharkas, Toulouse, Savin, JCP, 2011

Sharkas, Toulouse, Maschio, Civalleri, JCP, submitted

Range-separated hybrids (lrRPA+srDFT)

Based on a **range separation** of e-e interaction

$$E_{\text{exact}} = \min_{\Psi} \left\{ \langle \Psi | \hat{T} + \hat{V}_{ne} + \hat{W}_{ee}^{\text{lr}} | \Psi \rangle + E_{\text{Hxc}}^{\text{sr}}[n_{\Psi}] \right\}$$

long-range
interaction

$$\sum_{i < j} \frac{\text{erf}(\mu r_{ij})}{r_{ij}}$$

short-range
density functional

Savin, in *Recent developments and applications of modern DFT*, 1996

Toulouse, Colonna, Savin, PRA, 2004

- Single-determinant approximation:

$$E_0 = \min_{\Phi} \left\{ \langle \Phi | \hat{T} + \hat{V}_{ne} + \hat{W}_{ee}^{\text{lr}} | \Phi \rangle + E_{\text{Hxc}}^{\text{sr}}[n_{\Phi}] \right\}$$

This is a hybrid DFT with HF exchange at long range

srLDA
srPBE, etc...

- All what is missing is the **long-range correlation energy**:

$$E_{\text{exact}} = E_0 + E_c^{\text{lr}}$$

lrMP2
lrRPA

Ángyán, Gerber, Savin, Toulouse, PRA, 2005

Toulouse, Gerber, Jansen, Savin, Ángyán, PRL, 2009

lrRPA variants from ring coupled cluster doubles

- **dRPA** = direct ring CCD (without exchange):

$$E_{c,dRPA}^{lr} = \frac{1}{2} \text{tr} [\mathbf{w}_{ee}^{lr} \mathbf{T}_{drCCD}^{lr}]$$

$$= \text{diagram 1} + \text{diagram 2} + \dots$$

Scuseria, Henderson, Sorensen, JCP, 2008

- **RPAX-SO2** = ring CCD with exchange (Szabo-Ostlund's variant)

$$E_{c,RPAX-SO2}^{lr} = \frac{1}{2} \text{tr} [\mathbf{w}_{ee}^{lr} \mathbf{T}_{rCCDx}^{lr}]$$

$$= \text{diagram 1} + \text{diagram 2} + \text{diagram 3} + \text{diagram 4} + \text{diagram 5} + \text{diagram 6} + \dots$$

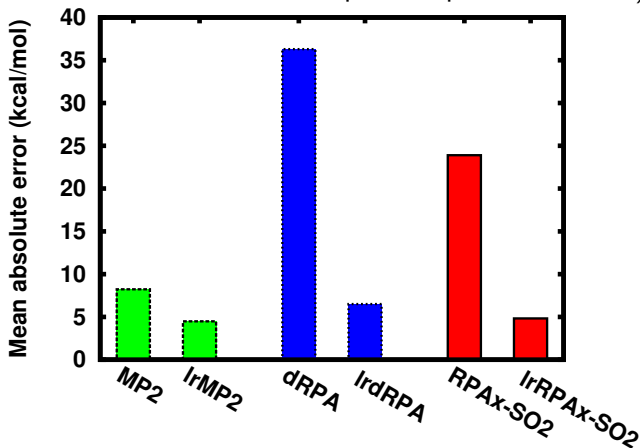
Heßelmann, JCP, 2011

Toulouse, Zhu, Savin, Jansen, Ángyán, JCP, 2011

Test of IrRPA+srDFT on atomization energies

AE6 set: 6 atomization energies of small molecules

($\mu = 0.5 \text{ bohr}^{-1}$, srPBE functional, cc-pVQZ, spin unrestricted):



⇒ Range separation improves the accuracy for all methods

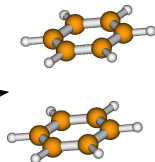
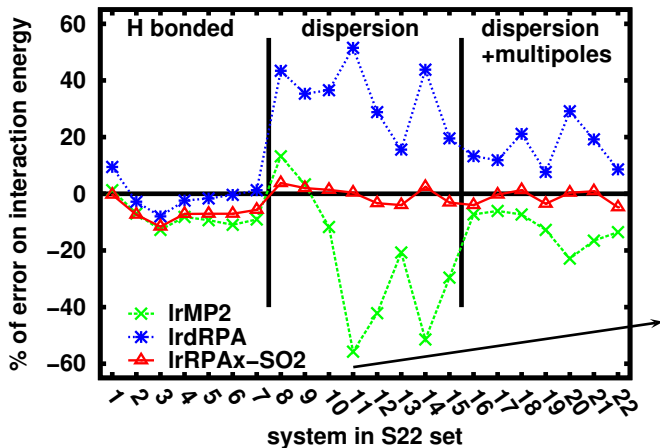
⇒ All range-separated methods give a MAE of about 5 kcal/mol

Mussard, Reinhardt, Luppi, Ángyán, Toulouse, in prep.

Test of IrRPA+srDFT on weak intermolecular interactions

S22 set: 22 equilibrium interaction energies of weakly-interacting molecular systems from water dimer to DNA base pairs

($\mu = 0.5 \text{ bohr}^{-1}$, srPBE functional, aug-cc-pVDZ):



⇒ IrRPAx-SO2/aVDZ gives a MAE of $\sim 4\%$ wrt CCSD(T)/CBS

Time-dependent range-separated hybrids

Linear-response TDDFT equation

$$\chi^{-1}(\omega) = \chi_0^{-1}(\omega) - f_{\text{Hxc}}(\omega)$$

⇒ excitation energies, linear-response properties

- Range separation for exchange kernel is now standard:

$$f_{\text{xc}} = f_{\text{x}}^{\text{lr,HF}} + f_{\text{x}}^{\text{sr,DFT}} + f_{\text{c}}^{\text{DFT}}$$


Tawada, Tsuneda, Yanagisawa, Yanai, Hirao, JCP, 2004

- Here, **range separation for both exchange and correlation kernels**:
Start with lrMP2+srDFT scheme for ground state:

$$E_{\text{xc}} = E_{\text{x}}^{\text{lr,HF}} + E_{\text{x}}^{\text{sr,DFT}} + E_{\text{c}}^{\text{lr,MP2}}$$

$$f_{\text{xc}} = f_{\text{x}}^{\text{lr,HF}} + f_{\text{xc}}^{\text{sr,DFT}} + f_{\text{c}}^{\text{lr,(2)}}(\omega)$$

linear
response



Rebolini, Savin, Toulouse, MP, 2013; Rebolini, Savin, Toulouse, in prep.

Other similar schemes: Pernal, JCP, 2012; Fromager, Knecht, Jensen, JCP, 2013;
Hedegård, Heiden, Knecht, Fromager, Jensen, JCP, 2013

Second-order correlation self-energy and kernel

$$\begin{aligned}
 & \frac{\delta}{\delta G_0(1,2)} \quad \frac{\delta}{\delta G_0(3,4)} \\
 & \quad \quad \quad E_c^{\text{MP2}} = \text{Diagram 1} + \text{Diagram 2} \\
 & \quad \quad \quad \Sigma_c^{(2)}(2,1) = \text{Diagram 3} + \text{Diagram 4} \\
 & \quad \quad \quad \Xi_c^{(2)}(2,4;1,3) = \text{Diagram 5} + \text{Diagram 6} \\
 & + \text{Diagram 7} + \text{Diagram 8} + \text{Diagram 9} + \text{Diagram 10}
 \end{aligned}$$

The diagrams represent second-order correlation self-energy and kernel terms. They are constructed from solid lines (representing occupied orbitals) and dashed lines (representing virtual orbitals). Arrows indicate the direction of electron flow.

- Diagram 1:** Two separate loops, each with a solid line and a dashed line.
- Diagram 2:** A single loop with two solid lines and two dashed lines, connected by two crossing lines.
- Diagram 3:** A loop with a solid line and a dashed line, connected to a vertex labeled 1 and 2.
- Diagram 4:** A loop with a solid line and a dashed line, connected to a vertex labeled 1 and 2, with an additional solid line connecting the two vertices.
- Diagram 5:** A loop with a solid line and a dashed line, connected to a vertex labeled 1, 2, 3, and 4.
- Diagram 6:** A loop with a solid line and a dashed line, connected to a vertex labeled 1, 2, 3, and 4, with an additional solid line connecting the two vertices.
- Diagram 7:** A loop with a solid line and a dashed line, connected to a vertex labeled 1 and 2.
- Diagram 8:** A loop with a solid line and a dashed line, connected to a vertex labeled 1 and 2, with an additional solid line connecting the two vertices.
- Diagram 9:** A loop with a solid line and a dashed line, connected to a vertex labeled 1 and 2.
- Diagram 10:** A loop with a solid line and a dashed line, connected to a vertex labeled 1 and 2, with an additional solid line connecting the two vertices.

In an orbital basis

- Long-range second-order correlation kernel (lrBSE2):

$$f_{c,ia,jb}^{\text{lr},(2)}(\omega) = - \sum_{k,c} \frac{\langle jk || ic \rangle^{\text{lr}} \langle ca || kb \rangle^{\text{lr}}}{\omega - (\varepsilon_a + \varepsilon_c - \varepsilon_k - \varepsilon_j)} - \sum_{k,c} \frac{\langle jc || ik \rangle^{\text{lr}} \langle ka || cb \rangle^{\text{lr}}}{\omega - (\varepsilon_b + \varepsilon_c - \varepsilon_i - \varepsilon_k)} \\ + \frac{1}{2} \sum_{c,d} \frac{\langle cd || ib \rangle^{\text{lr}} \langle ja || dc \rangle^{\text{lr}}}{\omega - (\varepsilon_c + \varepsilon_d - \varepsilon_j - \varepsilon_i)} + \frac{1}{2} \sum_{k,l} \frac{\langle kl || ib \rangle^{\text{lr}} \langle ja || lk \rangle^{\text{lr}}}{\omega - (\varepsilon_b + \varepsilon_a - \varepsilon_k - \varepsilon_l)}$$

⇒ The correlation kernel can be large when ω is close to a double excitation energy.

- Calculation of excitation energies in two steps:

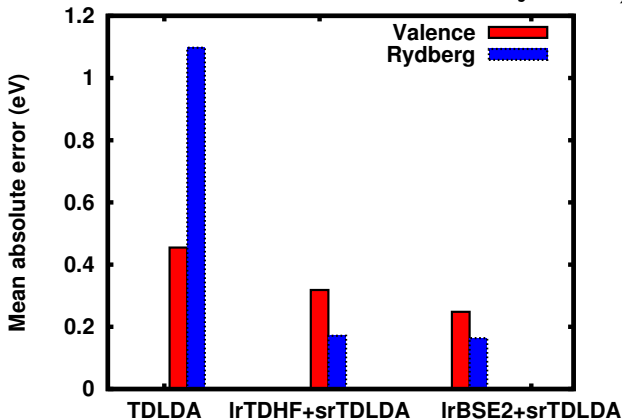
- 1 IrTDHF+srTDLDA calculation in the TDA: $\mathbf{A} \mathbf{X}_0 = \omega_0 \mathbf{X}_0$
- 2 perturbative addition of lrBSE2 kernel: $\omega = \omega_0 + \mathbf{X}_0^\dagger \mathbf{f}_c^{\text{lr},(2)}(\omega_0) \mathbf{X}_0$

Zhang, Steinmann, Yang, JCP, 2013

Rebolini, Savin, Toulouse, in prep.

Test of IrBSE2+srTDDFT on excitation energies

56 singlet and triplet excitation energies of 4 small molecules N_2 , CO , H_2CO , C_2H_4 ($\mu = 0.35 \text{ bohr}^{-1}$, srLDA functional, TDA, Sadlej+ basis):



⇒ For these systems, IrBSE2+srTDLDA does not improve much over IrTDHF+srTDLDA

Summary

Multiconfigurational hybrids (MCSCF+DFT)

- extension of usual hybrid functionals with explicit static correlation
- we still need to improve the functional

Double hybrids (MP2+DFT)

- we provided a theoretical derivation of one-parameter double hybrids
- reach near-chemical accuracy when static correlation not important

Range-separated hybrids (lrRPA+srDFT)

- fast basis convergence
- important to include exchange terms for dispersion interactions

Time-dependent range-separated hybrids (lrBSE2+srTDDFT)

- frequency-dependent second-order long-range correlation kernel
- more tests needed, in particular for effect of double excitations